MINIMIZATION OF ELASTIC THERMAL STRESSES DURING LASER MACHINING OF CERAMICS USING A DUAL-BEAM ARRANGEMENT

Michael F. Modest
Department of Mechanical Engineering
The Pennsylvania State University
University Park, PA 16802

Abstract

Lasers are emerging as a valuable tool for shaping and cutting hard and brittle ceramics. Unfortunately, the large, concentrated heat flux rates that allow the laser to efficiently cut and shape the ceramic also result in large localized thermal stresses in a small heat-affected zone. These notable thermal stresses can lead to micro-cracks, a decrease in strength and fatigue life, and possibly catastrophic failure. In order to assess where, when, and what stresses occur during laser scribing, an elastic stress model has been incorporated into a two-dimensional drilling as well as a three-dimensional scribing and cutting code. The results of the analysis for a single Gaussian laser source show that substantial tensile stresses develop over a thick layer below and parallel to the surface, which may be the cause of experimentally observed subsurface cracks. In this work the effect of splitting the beam into two parts is discussed: a highly-focussed beam that does the actual drilling or scribing, and a partially defocussed beam, used to heat the material ahead of, around, or behind the laser beam. Different secondary beam scenarios are investigated, and their effect on reducing the damaging tensile stresses is evaluated.

Introduction

Nearly all ceramics can be efficiently drilled, scribed or cut with a laser, although massive problems remain that are poorly, or not at all, understood. These problems include thermal stress, redeposition of evaporated or liquified material, poor surface finish, undesirable hole and groove tapers, etc. It is well known that laser irradiation causes damage in ceramics due to thermal stresses, resulting in micro-cracks and, often, catastrophic failure; in all cases laser processing severely reduces the bending strength of the ceramic (Copley et al. [1], Yamamoto and Yamamoto [2], deBastiani, Modest and Stubican [3]).

Criteria for stress failure of ceramics have been discussed in detail by Hasselman and Singh [4]. They note that ceramic materials will exhibit creep by diffusional processes at levels of temperature at which vacancy concentrations and mobility become appreciable. These temperatures correspond to about 0.5 to $0.7 \times T_{\text{melt}}$ of the material, resulting in very slow creep rates. At the fast heating rates during laser machining, creep rates fast enough to effect appreciable stress relaxation will not occur until much higher temperature levels, i.e., very close to the melting/decomposition temperature, are reached. A comprehensive literature review dealing with thermal stress behavior and creep of ceramics, as well as theoretical predictions of thermal stresses relevant to laser materials processing has been given in previous papers by the author [5, 6] and will not be repeated here.

In the previous papers our two-dimensional drilling [5] and three-dimensional cutting/scribing codes [6] were augmented by an elastic and viscoelastic (2D drilling only) stress model, which allows prediction of thermal stresses as they develop and decay during CW and pulsed laser drilling and scribing of ceramics. It was observed that during drilling substantial hoop and normal tensile stresses develop over a thick layer below and parallel to the surface, which may be the cause for experimentally observed subsurface cracks. It was also found that viscoelastic effects (treating the viscosity of the ceramic as temperature-dependent) were mostly limited to an extremely thin layer near the ablation front, where the ceramic has softened, relaxing compressive stresses during heating, followed by strong

tensile stresses during cooling. Thus is appears safe to neglect non-elastic stress behavior during laser machining of ceramics. Stress behavior during scribing was found to be quite similar, with maximum tensile stresses just ahead, and a crescent of tensile stresses surrounding the laser (front and sides).

It has been suggested that these damaging tensile stresses could perhaps be reduced, and stress damage be avoided, by using a secondary, semi-focussed laser beam to heat the surrounding material, thus eliminating the sharpest temperature gradients. In this paper we investigate, using our previous models [5, 6], whether and how the damaging thermal tensile stresses during laser machining can be reduced using such a dual beam arrangement. Several CW and pulsed drilling scenarios are discussed (the latter with a CW or pulsed secondary beam). Typical scribing operations are also discussed, to investigate the effects of displacing the center of the secondary beam from the primary beam (secondary heating ahead of or behind the laser).

Theoretical Background

Modest [7] used several assumptions in order to obtain a realistic, yet mathematically simple description of the laser drilling and scribing processes. Although the heat transfer codes allow for many scenarios, the following assumptions have been used in the elastic stress model implemented in both codes:

1. The solid is isotropic, has constant density, and is opaque, i.e., the laser beam does not penetrate appreciably into the solid.
2. The solid moves with constant velocity (scribing only).
3. Change of phase from solid to vapor occurs in a single step with a rate governed by a single Arrhenius relation.
4. The evaporated material does not interfere with the incoming laser beam (or is removed by an external gas jet).
5. The heat transfer properties are temperature independent.
6. Multiple reflections of laser radiation within the groove are neglected, restricting the model to shallow holes, holes with steep sidewalls, or material with high absorptivity.
7. Heat transfer is unaffected by thermal expansion (always true for opaque ceramics as shown by an order of magnitude analysis).

In addition the following assumptions are made for the stress calculations:

1. The mechanical properties, such as the modulus of elasticity, are temperature independent.
2. Displacements are small quantities that vary over the entire volume. Large displacements, such as buckling of thin plates are not allowed.
3. No external forces are applied to the solid. Stresses occur only due to thermal expansion or contraction.
4. Inertia effects are negligible during stress development (always true of opaque ceramics, but may break down for semitransparent ceramics subjected to ns laser pulsing).

Heat Transfer The transient heat conduction equation is solved numerically for the entire workpiece of dimensions $L \times W \times H$, irradiated by two concentric or displaced Gaussian laser beams on its top surface. The four side surfaces are assumed insulated (since the workpiece is generally only a small part of a larger specimen), while top and bottom surface experience convection and radiation losses. Recession of the top surface due to the laser irradiation is modeled through a single-step Arrhenius rate equation. The resulting non-dimensional set of non-linear moving-boundary problem is solved using boundary-fitted coordinates together with a structured grid. Details of the heat transfer model can be found in Roy and Modest [8] and, to a lesser extent in Modest [6]. Relevant non-dimensional parameters governing the heat transfer are

$$N_k = \frac{k\,(T_{\mathrm{re}} - T_\infty)}{F_0 w_0}, \qquad \mathrm{Ste} = \frac{\Delta h_{\mathrm{re}}}{c_p\,(T_{\mathrm{re}} - T_\infty)}, \qquad U = \frac{u w_0}{(k/\rho c_p)}, \tag{1}$$

where $\rho, c_p, k, \Delta h_{\text{re}}$ are the density, specific heat, thermal conductivity and "heat of removal" of the material, F_0 and w_0 are laser intensity at the center of the beam and the $1/e^2$ beam radius, respectively, for the primary beam, while u is the scanning speed of both lasers. Finally, T_∞ and T_{re} are the temperatures of the environment and at the ablation/decomposition point of the material respectively.

Thermal Stresses The extreme temperature gradients that occur during laser machining result in large, localized thermal expansion. This thermal expansion, in turn, causes large thermal stresses in the ceramic. While under most conditions ceramics may be considered elastic, during laser machining there will be a thin zone near the receding surface where significant creep may occur. The influence of the thin creep zone near the top surface will be neglected here, since its contribution to the overall stress field is expected to be small [5].

Under the conditions given by the heat transfer portion, the stress distribution is solved using the standard set of equations for an elastic body with constant properties. No-traction boundary conditions are applied to the top and bottom surfaces, while—in general—all side surfaces are assumed clamped. This assumption is made since the workpiece for the numerical analysis is usually only a small part of a much larger specimen, which remains cold and unstressed away from the laser. This assumption is tested by performing calculations on workpieces of varying dimensions, making sure that the stress field remains the same. One exception to the use of clamped sides is the case when the laser scans onto (or off) a workpiece, in which case the corresponding side surface is given a no-traction condition. The stress equations are solved in non-dimensional form on the same structured, body-fitted grid that is used for the heat transfer calculations. Non-dimensional stresses $\underline{\underline{\sigma}}$ are then found as

$$\underline{\underline{\sigma}} = \frac{\bar{\underline{\underline{\sigma}}}}{2\mu\alpha(T_{\text{re}} - T_\infty)} \tag{2}$$

where μ is Lamé's elastic constant (= G, the shear modulus), ν is Poisson's ratio, and α is the coefficient of linear expansion.

Results and Discussion

In order to assess the potential to minimize thermal stresses with a dual laser beam arrangement, a large number of drilling and scribing simulations have been carried, and a small selection of typical results will be presented here. All cases presented here are modeled using the physical properties of silicon carbide together with a typical CO_2 laser with a $w_0 = 175\mu$m radius; however, since all calculations and results are in non-dimensional form, they apply equally to all other ceramics, such as silicon nitride or alumina.

All drilling results shown in Figs. 1 through 7 use laser parameters of Ste = 3.3 and $N_k = 0.01$, which—in the case of silicon carbide—corresponds roughly to 600W total absorbed power with a 175μm beam. Stress results are rather insensitive to the value of the Stefan number (which is unique to a material), while different values of N_k can be interpreted as pertaining to a different material and/or different laser power and beam radius. Several other values of N_k (Smaller and larger), were considered, which—while producing slightly different stress levels—all showed the same trends. Figures 1 through 4 show typical results for CW drilling of a piece of ceramic. To understand when and where damaging tensile stresses occur, Fig. 1 shows the development of the maximum principal stress field as a function of time during the drilling process. At all times there is a strongly compressive zone right below the surface, followed by a tensile layer deeper inside. At small times (i.e., well before the laser punches through the workpiece) the maximum tensile stress is located right beneath the lip of the hole, where the surface of the hole is convex. The convexness of the material's surface makes it more difficult for heat to diffuse inside, thus thickening the heat-affected zone and, apparently, also the tensile stress layer. As time goes on, and the hole becomes deeper, the tensile layer moves further from the center and becomes larger, going deeper into the material (again, following the development of the heat-affected zone). Shortly before the material is drilled through, a lot of heat is stored directly below the laser (since it can no longer diffuse into the material), causing very strong tensile stresses (probably leading to explosive drill-through behavior). After drill-through the two tensile stress lobes grow together to form a crescent as seen from the "steady-state" picture (i.e., when no more material removal takes place, and laser irradiation is essentially balanced by convection and re-radiation losses).

Figure 2 shows the maximum value of the tensile stress inside the tensile lobe below the lip of the hole (or, rather, the maximum value at a node center, which leads to the jaggedness displayed by the lines) as a function of time. A

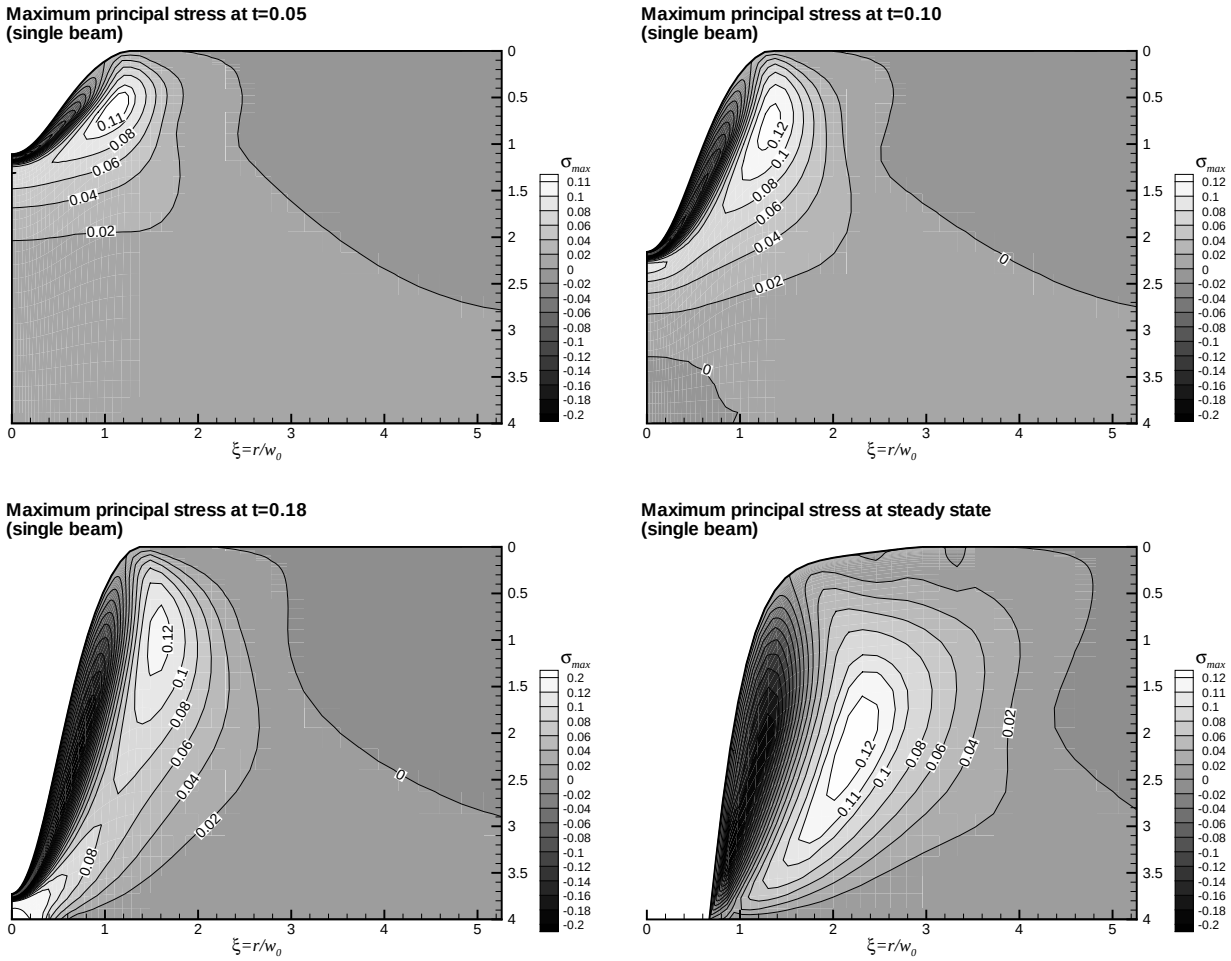

Figure 1: Transient development of maximum principal stresses during single-beam CW laser drilling

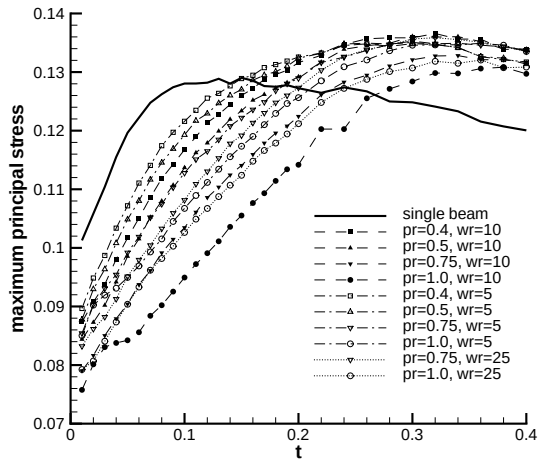

Figure 2: Transient maximum principal stresses during CW laser drilling using various dual-beam arrangements

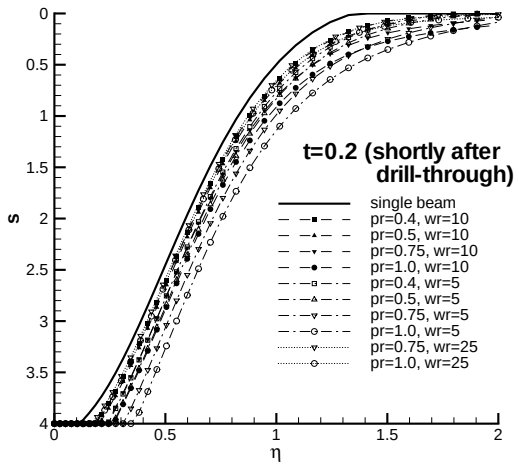

Figure 3: Hole profile during CW laser drilling shortly after drill-through using various dual-beam arrangements

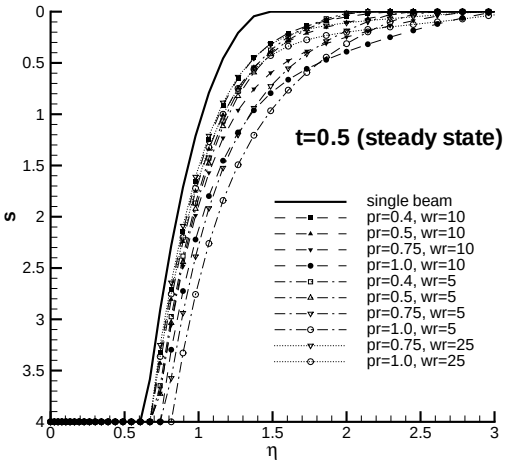

Figure 4: Quasi-steady state hole profile during CW laser drilling using various dual-beam arrangements

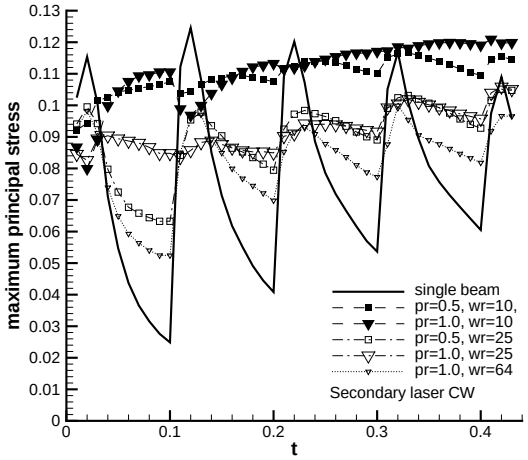

Figure 5: Transient maximum principal stresses during pulsed laser drilling using various CW secondary beam arrangements

number of scenarios have been considered with power ratios $pr = P_2/P_1$ ranging from 0.4 to 1.0, and beam ratios varying from $wr = (w_{02}/w_{01})^2 = 5$ to 25. All dual beam arrangements lead to somewhat lower tensile stresses (10-25%) for short times. However, when the process nears drill-through conditions, stresses from the dual-beam arrangement catch up, and eventually exceed the single-beam stresses, apparently due to the excess in heat deposited in the peripheral material. While few actual drillings would be carried out much beyond drill-through, one must realize that the early reductions in stress are rather minor, and probably not sufficient to prevent stress damage during the drilling process. It is interesting to note that an optimum radius exists for the secondary beam: for all power levels the largest reduction of maximum stress occurs with the intermediate beam radius ratio of $wr = 10$. On the other hand, stress levels continuously decrease with increasing power ratio. However, this benefit comes at a price, as seen from Figs. 3 and 4 the semi-focused secondary beam increases the taper of hole. This effect is not too pronounced until shortly after drill-through (essentially widening the hole a bit, rather than increasing its taper, in particular for small *wr*), but becomes pronounced if the drilling process is continued until steady-state (in particular for large *wr* and/or *pr*).

To assess the potential of dual-beam arrangements for pulsed drilling, the same values of $N_k = 0.01$ and Ste =3.3 are employed again (now indicating an *average* absorbed power of 600W). The laser is assumed to have a duty cycle of 25% (i.e., it is on during 25% of the time with 4 × average power, and off 75% of the time). Total pulse duration in non-dimensional time is 0.1 (or 0.75 ms for the indicated SiC conditions); thus, the laser is firing for times $0 < t < 0.025$, $0.1 < t < 0.125$, etc., producing the sharp peaks and valleys in maximum tensile stresses shown in Fig. 5. Note that, despite the larger peak power, the maximum stresses are not larger than during CW drilling. Note also that differences between maxima and minima decrease with time, because the material retains more and more heat between pulses.

Two different types of dual-beam arrangements are considered; in the first one the secondary beam runs in CW mode (requiring a second laser), and in the other arrangement the secondary beam is also pulsed (same frequency and duty cycle, as obtained by splitting the beam from a single laser). During single-beam pulsed drilling a relatively thin lobe of tensile stresses develops below the lip of the hole oriented more or less parallel to the vertical surface of the hole. During the second (and later) pulse a second tensile zone develops below the center of the laser. During cooling, i.e., when the laser is off between pulses, the two lobes combine to form a large crescent parallel to the hole's surface. Qualitatively, this behavior is very similar to the CW behavior shown in Fig. 1. If a dual beam arrangement is used, with the secondary beam running in CW mode, the continuous heating of the material results in fairly uniform maximum tensile stresses in time. However, if the secondary beam power is too concentrated ($wr = 10$), this uniform maximum stress is essentially as high as the highest peak stress encountered during single beam drilling. Also due to the more uniform heating the tensile stress lobe becomes a lot wider and is oriented parallel to the top surface,

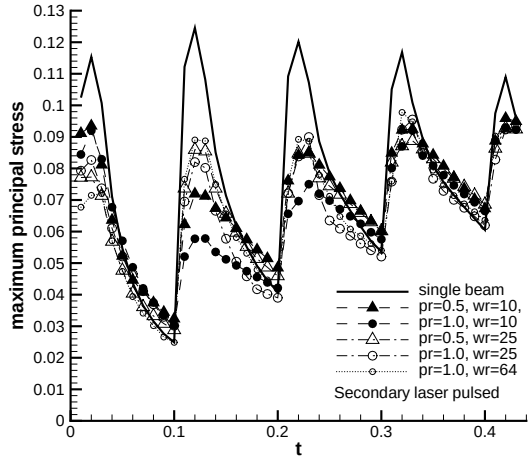

Figure 6: Transient maximum principal stresses during pulsed laser drilling using various pulsed secondary beam arrangements

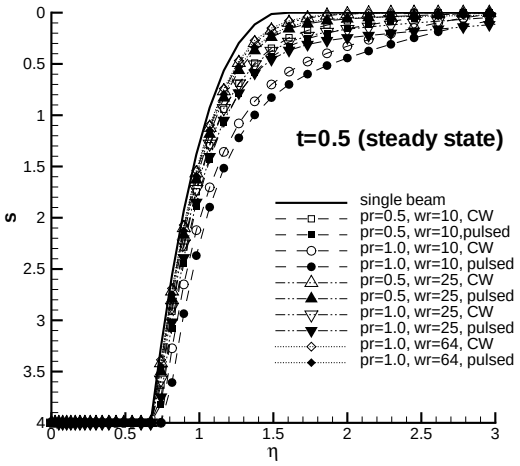

Figure 7: Quasi-steady state hole profile during pulsed laser drilling using various dual-beam arrangements

extending beyond the lip (i.e., the lobe is lying "flat"). For a more defocussed secondary beam ($wr = 25$), the fairly constant-in-time maximum stress is substantially below peak stress levels for single-beam drilling ($\simeq 30\%$); suppression of the cyclical stress pattern can also be expected to suppress some stress damage.

If the secondary beam is also pulsed, at the same frequency as the primary beam, the behavior is similar to single beam pulsed drilling: two strong lobes of tensile stresses form, during laser-on time, under the lip of the hole and under the bottom of the hole, growing together after the laser is turned off; however, a third tensile lobe forms deep inside the material, parallel to the top surface. After the laser is turned off, this lobe also combines with the other two. As seen from Fig. 6 the pulsed secondary beam reduces peak stresses substantially and—like CW drilling—the peak stress increases with time, but—unlike CW drilling—the peak never catches up with the single-beam peak levels.

Of course, using a secondary beam again comes at a price, increasing hole diameter and taper, as shown in Fig.7. Not surprisingly, the secondary beam with the highest power density causes the worst taper ($pr = 1$, $wr = 10$, CW or pulsed); best results are obtained from the stress and hole geometry viewpoints around the conditions ($pr = 0.5$, $wr = 25$) and ($pr = 1$, $wr = 64$); defocussing the secondary laser beyond $wr = 64$ brings the performance closer again to single beam performance.

Typical scribing results are shown in Figs. 8 through 13. Non-dimensional parameters are essentially the same as for drilling, except N_k was changed to $N_k = 0.02$, (halving the power), and total non-dimensional pulse time was set to 0.25. Laser scanning speed was set to $U = 4.25$, corresponding to roughly 10 cm/s in the case of SiC. These parameters were chosen to avoid through-cutting (which the stress part of our 3D code is unable to treat at this time) and to conform with our previous paper on single-beam scribing [6]. As for drilling, different conditions were tested leading to very similar results.

Figure 8 shows maximum principal stresses for the single-beam CW scribing case: a crescent of tensile stresses — approximately normal to the materials surface — surrounds the laser in the front and to the sides. In addition, a lobe of tensile radial stresses extends from the interior tension region to the top surface. Figure 9 shows the same case, but with a concentric secondary beam with $pr = 0.5$ and $wr = 100$. It is observed that the relatively strong lobe of radial tensile stresses is gone, and that the strong normal stresses ahead of the laser have diminished considerably. However, the strong tensile stresses to the sides of the laser beam remain and, indeed, have increased a few percent (from $\sigma_{1,\max} = 0.130$ for a single beam, to $\sigma_{1,\max} = 0.136$ for dual beams). If the center of the secondary beam is moved ahead or behind the primary beam by a few primary beam radii, the stresses remain essentially unaffected (less than 2% change, not shown). If stronger and/or more focussed secondary beams are employed the results remain qualitatively the same, but maximum tensile stresses increase more substantially.

For pulsed scribing, as for pulsed drilling, CW as well as pulsed secondary beams were considered. Figure 10 shows the maximum principal stress distribution, for a single pulsed beam, just before the end of the 5th pulse,

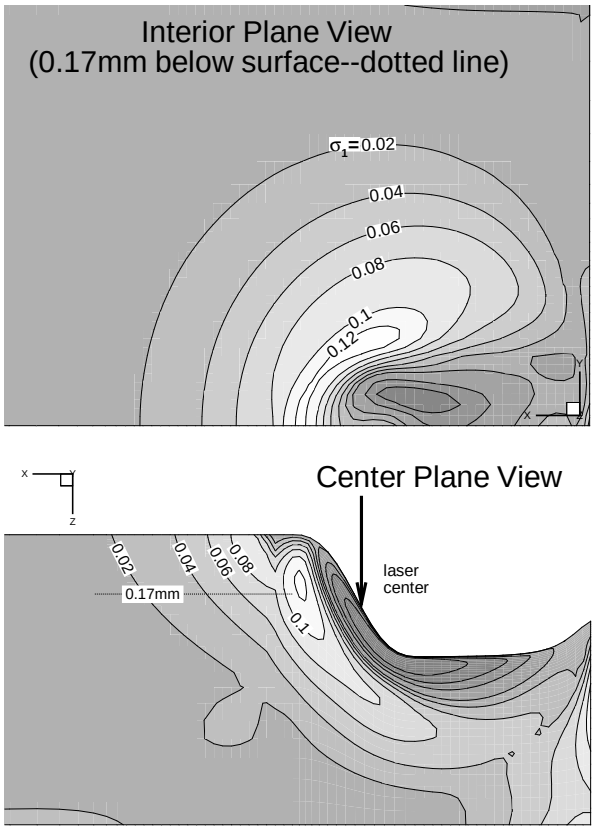

Figure 8: Maximum principal stress field during CW laser scribing using a single beam ($N_k = 0.02, U = 4.25$)

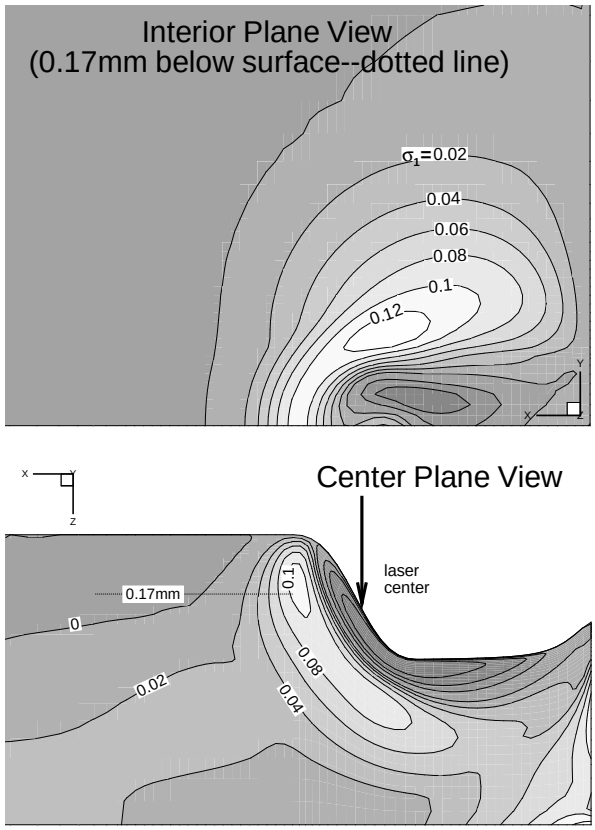

Figure 9: Maximum principal stress field during CW laser scribing using a dual-beam arrangement ($N_k = 0.02, U = 4.25, pr = 0.5, wr = 100$)

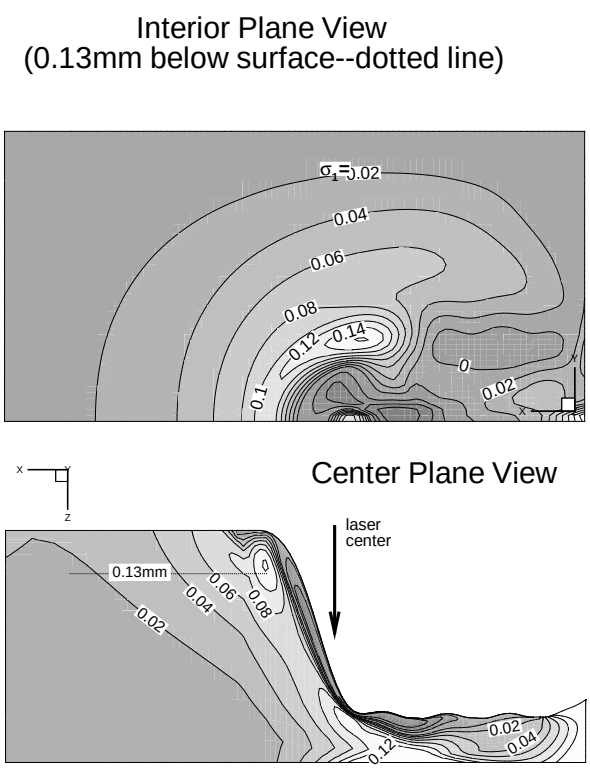

Figure 10: Maximum principal stress field during pulsed laser scribing using a single beam ($N_k = 0.02, \tau_p = 0.25, U = 4.25$)

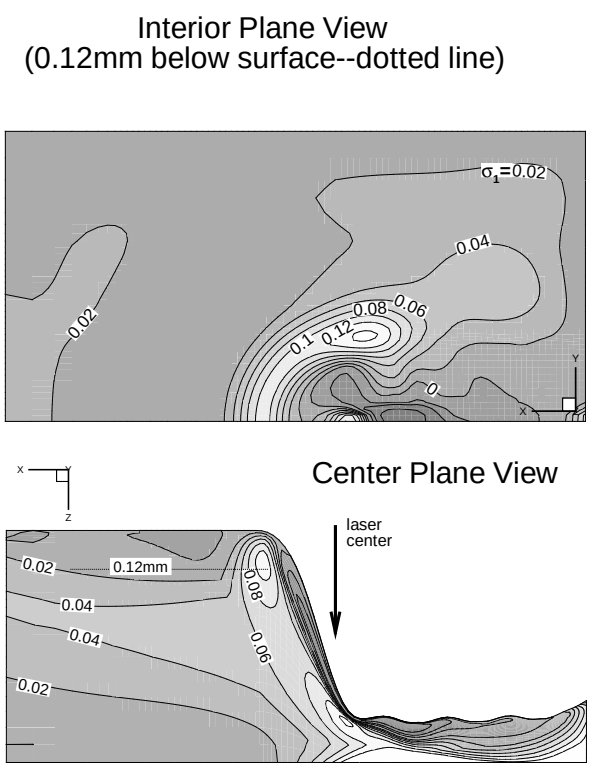

Figure 11: Maximum principal stress field during pulsed laser scribing using a CW secondary beam ($N_k = 0.02, \tau_p = 0.25, U = 4.25, pr = 0.5, wr = 100$)

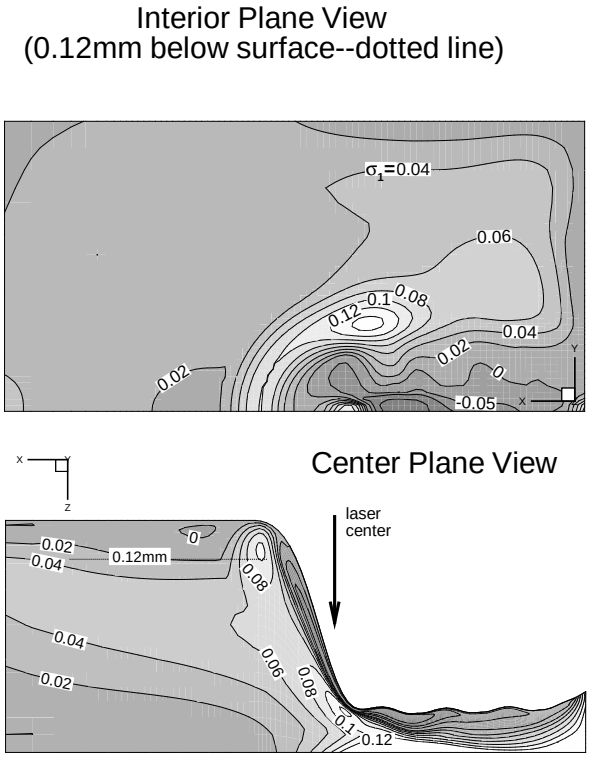

Figure 12: Maximum principal stress field during pulsed laser scribing using a pulsed secondary beam ($N_k = 0.02, \tau_p = 0.25, U = 4.25, pr = 0.5, wr = 100$)

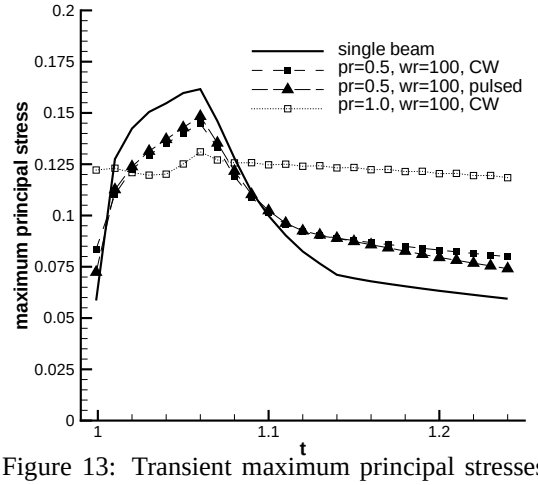

Figure 13: Transient maximum principal stresses during pulsed laser scribing with various secondary beam arrangements ($N_k = 0.02, \tau_p = 0.25, U = 4.25, pr = 0.5$ and 1, $wr = 100$)

$t = 1.06$ (i.e., when the largest thermal stresses occur). The behavior is rather similar to the CW case, i.e., maximum principal stresses are mostly in a direction normal to the surface, with a crescent forming around the front and to the sides of the laser; because of the thinner heat-affected layer the maximum stress is about 25% larger ($\sigma_{1,\max} = 0.162$). As for the CW case, there is a radial stress lobe going to the top surface in front of the laser. Two additional features in the pulsed case are (i) tensile stress build-up below the scribe (since the lesser conduction losses during pulsed scribing lead to almost cut-through conditions, trapping energy below the scribe), and (ii) little islands of tensil stresses along the sides of the scribe (because of small beam-overlap the ridge of the scribe has minor extrusions, again trapping energy; this effect is difficult to see in the figure shown here). In the presence of a secondary beam (Fig. 11 for a CW secondary beam, and Fig. 12 for a pulsed secondary beam) the radial stress lobe is removed (as in the CW case), and the maximum stresses in the crescent surrounding the scribe are reduced (to $\sigma_{1,\max} = 0.145$ and 0.148, respectively). Figure 13 compares transient development of the maximum tensile stresses in the side lobe during the 5th pulse for several scenarios. As for drilling, the secondary beam reduces maximum stresses during laser-on time ($1 < t < 1.0625$), while smoothing out the distribution during cool-down. For $pr = 0.5$ there is very little difference between CW and pulsed secondary beams. However, using a stronger CW secondary beam ($pr = 1$) leads to essentially flat maximum tensile stresses, substantially reduced from the maximum value using single-beam scribing.

Summary and Conclusions

The possibility of minimizing thermal stresses, as they occur during laser machining of ceramics, through the use of a dual beam arrangement was investigated. The basic idea is that, by superimposing a secondary, semi-focussed beam on top of the primary, focussed beam, additional heating will take place in the surrounding material, thus eliminating the sharpest temperature gradients and, consequently, the strongest thermal stresses. Several CW and pulsed drilling

arrangements as well as typical scribing operations were investigated.

Overall, the results of this research were somewhat disappointing since, during drilling, no dual-beam arrangement (different power levels, different focussing levels) was able to reduce the maximum tensile stresses by much more than 30% or so. Still, such amounts of stress relief can be the difference between damage and non-damage. During pulsed drilling a CW secondary beam was found to reduce not only maximum stresses, but also to essentially eliminate stress cycling between laser-on and laser-off times. Even a pulsed secondary beam can substantially reduce such stress cycling.

If was also found that, during CW scribing of ceramics, stresses were relatively unaffected by power and focussing levels of the secondary beam. Focussing the secondary beam ahead or behind the primary beam also had very little effect. The secondary beam was able to substantially reduce the tensile stresses occurring ahead of the moving laser, but was unable to reduce the stresses to the sides of the scanning laser. Results for pulsed scribing were similar, but — as for pulsed drilling — the strong tensile pockets to the sides of the scribe were reduced considerably.

Acknowledgments

Support by the National Science Foundation through Grant no. CMS-9634744 is gratefully acknowledged.

References

1. Copley, S. W., R. J. Wallace, and M. Bass (1983), Laser Shaping of Materials, In *Lasers in Materials Processing* (Edited by Metzbower, E. A.), American Society for Metals, Metals Park, Ohio.
2. Yamamoto, J., and Y. Yamamoto (1987), Laser Machining of Silicon Nitride, In *International Conference on Laser Advanced Materials Processing – Science and Applications*, 297–302. High Temperature Society of Japan, Japan Laser Processing Society, Osaka, Japan.
3. DeBastiani, D., M. F. Modest, and V. S. Stubican (1990), Mechanisms of Reactions During CO_2-Laser Processing of Silicon Carbide, **J. Amer. Cer. Soc. 73**(7), 1947–1952.
4. Hasselman, D. P. H., and J. P. Singh (1986), Criteria for the Thermal Stress Failure of Brittle Structural Ceramics, In *Thermal Stresses I* (Edited by Hetnarski, R. B.), Ch. 4, North-Holland, New York.
5. Modest, M. F. (1998), Transient Elastic and Viscoelastic Thermal Stresses During Laser Drilling of Ceramics, **J. Heat Transfer 120**, 892–898.
6. Modest, M. F., and T. M. Mallison (2000), Transient Elastic Thermal Stresses During Laser Scribing of Ceramics, **J. Heat Transfer**, accepted for publication.
7. Modest, M. F. (1996), Three-Dimensional, Transient Model for Laser Machining of Ablating/Decomposing Materials, **Int. J. Heat Mass Transfer 39**(2), 221–234.
8. Roy, S., and M. F. Modest (1993), CW Laser Machining of Hard Ceramics — Part I: Effects of Three-Dimensional Conduction and Variable Properties and Various Laser Parameters, **Int. J. Heat Mass Transfer 36**(14), 3515–3528.